STRUCTURE AND PROPERTIES OF MELT-SPUN Al-Zr-Ti ALLOYS II. THE SOLIDIFICATION MICROSTRUCTURE AND MICROHARDNESS

PŘEMYSL MÁLEK, MILOŠ JANEČEK, BOHUMIL SMOLA, PAVEL BARTUŠKA

Thin ribbons of the Al-Zr-Ti alloy with variable Zr:Ti ratio were prepared using the melt spinning method. The solidification microstructure was found to be inhomogeneous along the direction perpendicular to the ribbon plane and dependent on the Zr:Ti ratio. The phase composition was far from the phase equilibrium. However, second phase particles of the size below 10 nm were present especially in the Zr-rich alloys. They precipitated preferentially in a fan-shape morphology and electron diffraction identified most of them to be formed by the metastable $Al_3(Zr_xTi_{1-x})$ phase with the cubic $L1_2$ structure. The grains of the Ti-rich alloys were nearly free of such particles. The coarse particles present in the Ti-rich alloys were mostly constitutional particles in the spectrum of which Fe was found. The microhardness values were found much higher in the Zr-rich alloys. A correspondence between microhardness and solidification microstructure and phase composition was found.

K e y w o r d s : Al-based alloys for elevated temperatures, rapid solidification, solidification microstructure, electron microscopy, microhardness

STRUKTURA A VLASTNOSTI SLITIN Al-Zr-Ti PŘIPRAVENÝCH METODOU „MELT SPINNING" II. MIKROSTRUKTURA A MIKROTVRDOST PO TUHNUTÍ

Tenké pásky slitiny Al-Zr-Ti s proměnným poměrem Zr:Ti byly připraveny metodou nástřiku taveniny na rotující měděný válec. Ztuhlá struktura je nehomogenní podél směru kolmého k rovině pásku a závisí na poměru Zr:Ti. Fázové složení je daleko od termodynamické rovnováhy, ale částice druhé fáze s velikostí pod 10 nm byly nalezeny především ve

RNDr. P. Málek, CSc., RNDr. M. Janeček, CSc., Doc. RNDr. B. Smola, CSc., Department of Metal Physics, Charles University, Ke Karlovu 5, 121 16 Prague 2, Czech Republic.

Ing. P. Bartuška, CSc., Institute of Physics, Academy of Sciences of the Czech Republic, Na Slovance 2, 180 40 Prague 8, Czech Republic.

slitinách bohatých na Zr. Elektronová difrakce ukázala, že částice precipitující především ve vějířovité morfologii jsou tvořeny metastabilní fází $Al_3(Zr_xTi_{1-x})$ s kubickou $L1_2$ strukturou. Ve slitinách bohatých na Ti podobné částice nebyly nalezeny, pozorované hrubé částice byly tvořeny konstitučními fázemi obsahujícími Fe. Výrazně vyšší mikrotvrdost byla naměřena ve slitinách bohatých na Zr. Existuje korelace mezi mikrotvrdostí a mikrostrukturou a fázovým složením po tuhnutí.

1. Introduction

A high strength of aluminium alloys may be achieved by the formation of large volume fractions of small second phase particles. These particles may be formed either during the crystallisation or during subsequent thermal treatment. In both cases special chemical compositions and advanced preparation routes have to be used. In order to retain the high strength at elevated temperatures the particles have to be resistant to dissolution and coarsening.

There are three requirements relating to the chemical composition which must be met for the successful development of the elevated temperature Al-based alloys [1]:

– a capability of the additives to form intermetallic phases with Al which have a low lattice mismatch to the Al-matrix,

– a low equilibrium solid solubility of the additives up to the temperatures of 700 K in order to avoid the dissolution of strengthening phases,

– a low diffusivity of the additives in Al in order to slow down the diffusion controlled coarsening of particles of strengthening phases.

It has been shown that zirconium meets very well all these requirements – it is able to form the intermetallic Al_3Zr phase with a very low lattice mismatch to the Al-based matrix [1, 2], its maximum solid solubility reaches only 0.28 wt.% at 934 K [3], and its diffusion rate in Al is the slowest of all transition metals [4]. Several recent papers have shown that Ti atoms may substitute for Zr atoms in the lattice of the intermetallic Al_3Zr phase and reduce its lattice mismatch even to zero at a suitable Zr:Ti ratio [5, 6]. Consequently, even stronger resistance to particle coarsening may be expected in the ternary Al-Zr-Ti alloy [7, 8].

The Al-Zr-Ti system with a variable Zr and Ti content was chosen for our investigation. In order to avoid extensive segregation and formation of coarse primary particles during solidification the Al-Zr-Ti alloys were rapidly solidified using the chill block melt-spinning method. Rapid solidification techniques with quenching rates up to 10^6 $K \cdot s^{-1}$ were reported to extend the solid solubility limits of Zr and Ti up to 4.9 wt.% and 3.5 wt.%, respectively, [9] and to refine the solidification microstructure [10]. Both the phase composition and solidification microstructure depend on the solidification rate. Despite of a very small thickness of the as-melt-spun ribbons a gradient in the solidification rate arise along the direction perpendicular to the ribbon plane. The chemical composition was not found to be

influenced by this gradient [6]. However, the solidification microstructure is usually different at the cooled surface which was in contact with the rotating wheel and at the free surface (e.g. [10]). The main objective of our investigation was to study the solidification microstructure as a function of the Zr:Ti ratio, the structural inhomogeneities and their influence on microhardness.

2. Material and procedure

The thin Al-Zr-Ti ribbons with a variable Zr:Ti ratio were prepared using the melt-spinning method (for details see [6]). The nominal chemical compositions given in Table 1 were selected. They correspond to the equilibrium phase composition of Al-5vol.%$Al_3(Zr_xTi_{1-x})$ in a fully precipitated state with the stoichiometric parameters $x = 1, 0.75, 0.5, 0.25$, and 0. The analysis performed using the EDX and WDA methods revealed that the actual chemical composition was (within the experimental error of the analytical methods used) equal to the nominal composition and no significant gradient in the chemical composition was observed [6]. Despite the contents of Zr and Ti are below the reported extended solid solubility limits in Al, the as-prepared ribbons are not single phase materials. The X-ray methods confirmed the presence of second phase particles and identified these particles to be formed by the metastable $Al_3(Zr_xTi_{1-x})$ phase in the Zr-rich alloys ($x \geq 0.5$).

Table 1. Nominal chemical composition of the Al-$Al_3(Zr_xTi_{1-x})$ alloys in wt.%

x	1	0.75	0.5	0.25	0
Zr	4.1	3.1	2.1	1.0	–
Ti	–	0.55	1.1	1.65	2.2

The solidification microstructure was studied by using both the light and the scanning electron microscopy. The specimens for the light microscopy investigation were mounted in the resin, their longitudinal section was polished mechanically and electrolytically in the solution of 20% $HClO_4$ and 80% ethanol at 253 K and 30 V, and etched chemically in the Dix-Keller etching solution. The scanning electron microscopy investigation was performed on the surfaces of the as-melt-spun ribbons and on the transversal sections as well. In the latter case the ribbons were covered electrolytically by pure Ni, mounted and polished mechanically or electrolytically (20% $HClO_4$, 80% ethanol at 243 K and 15 V).

The Knoop microhardness was measured at room temperature on the metallographically polished longitudinal sections using a LECO M-400-A microhardness tester at the load of 10 g and dwell time of 15 s. At least 20 measurements were

performed for each specimen. Some specimens were slightly etched prior to microhardness measurements to allow the correlation of the microhardness value with the structure.

The internal microstructure was studied by means of the transmission electron microscopy. The ribbons were thinned electrolytically in the 66% HNO_3 – 33% CH_3OH solution. The observations were carried out using the analytical electron microscope JEOL 2000 FX at 200 kV.

3. Experimental results

No particles were observed at the chilled surface except for the Al-Ti alloy where relatively coarse (up to 10 μm) oval particles were observed. The presence of Fe was found in the spectrum taken from these particles. Numerous light particles inhomogeneously distributed within the structure were observed at the free surface of all materials. Their size was usually between 1 and 5 μm and a slight peak of oxygen was found in their spectrum. A fine grained structure with the equiaxed grains of the size about 1 μm was observed in regions containing less particles (Fig. 1).

The solidification microstructure is not homogeneous along the direction perpendicular to the ribbon plane (Fig. 2). A zone of columnar grains with the width

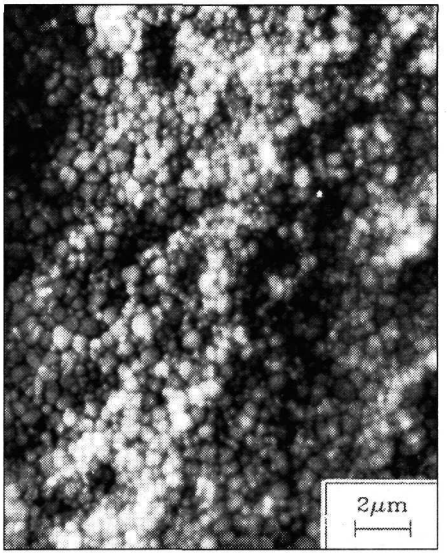

Fig. 1. The microstructure of a free surface in the as melt-spun Al-Zr-Ti ribbon, $x = 0.75$, SEM.

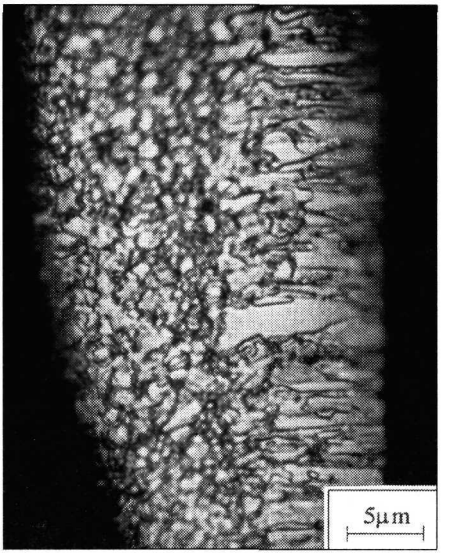

Fig. 2. The grain structure of the Al-Zr-Ti alloy, $x = 0.5$, light microscopy.

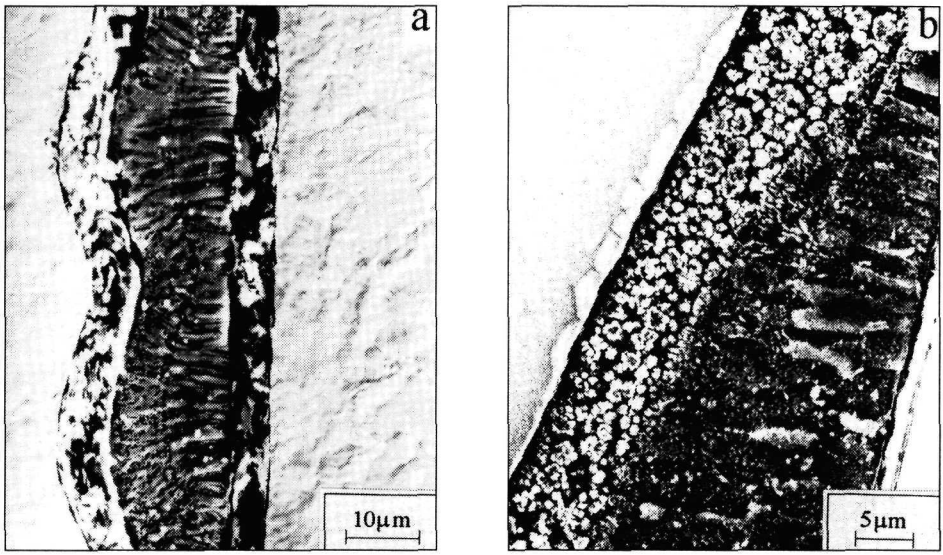

Fig. 3. The grain structure of the Al-Zr-Ti alloys revealed on the longitudinal section of ribbons (SEM): a) Al-Zr alloy, b) Al-Ti alloy.

of about 1 μm and the length of about 10 μm was observed at the chilled surface of all materials. The width of this zone extends usually to the middle of the ribbon. However, it may even disappear at places with a smaller ribbon thickness (Fig. 3a). A fine microcellular structure was observed in some columnar grains in the Al-Ti alloy (Fig. 3b). The zone adjoining the free surface exhibits a cellular structure with the mean size of individual equiaxed cells of about 1 μm in the Zr-rich alloys ($x \geq 0.5$) (Fig. 2). Numerous regions with the petal-like morphology were observed in the Ti-rich alloys ($x \leq 0.25$) (Fig. 3b).

Mechanical properties were characterised by Knoop microhardness (*HK*). Table 2 presents the mean *HK* values measured in the as-melt-spun ribbons. Each of these mean values represents the average from at least 20 measurements. It is obvious that the microhardness is much higher in the Zr-rich alloys than in the Ti-rich ones. The former alloys exhibit a much broader scatter in the *HK* values (e.g. values between $HK = 70$ and 154 were measured in the binary Al-Zr alloy). A detailed investigation was performed to identify the reasons of this scatter. It was found that statistically higher values of Knoop microhardness were measured at places with larger ribbon thickness. At thicker places the indents were applied at various distances from the chilled surface. The highest values were

Table 2. Knoop microhardness in the as melt-spun ribbons of the Al-$Al_3(Zr_xTi_{1-x})$ alloys

x	1	0.75	0.5	0.25	0
HK [kg/mm^2]	103 ± 22	112 ± 15	110 ± 25	62 ± 3	48 ± 6

found in the middle of the ribbon, the lowest values close to the chilled surface. A correlation with the solidification microstructure revealed statistically lower values of microhardness in the zone of columnar grains (Fig. 4).

The above given results suggest significant differences between the Zr-rich and Ti-rich alloys. Moreover, TEM experiments also confirmed differences in the internal microstructure. Fig. 5a shows the typical microstructure of the Zr-rich alloys at low magnification. The mean grain size evaluated from micrographs is below 1 μm in all these alloys. The interfaces exhibit a marked curvature. A slightly coarser microstructure with the mean grain size of about 2 μm was found in Ti-rich alloys (Fig. 5b). The most interfaces are straight and meet at triple points characterised by dihedral angles close to the equilibrium value of 120°.

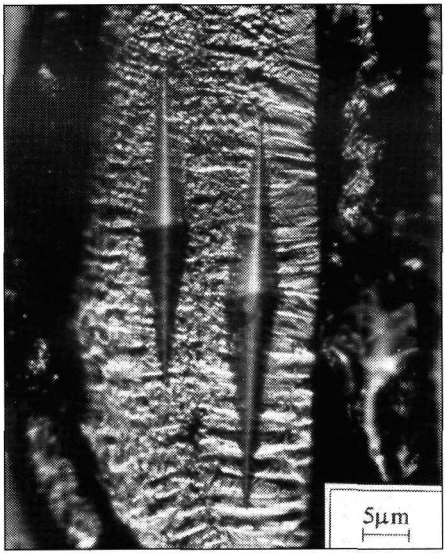

Fig. 4. The influence of the solidification structure on Knoop microhardness, Al-Zr alloy (OM).

A typical feature of Zr-rich alloys is the presence of two types of particles – very fine particles (below 4 nm) arranged into a fan shaped morphology (Fig. 6a) and individual coarser (about 10 nm), probably spherical particles located both between the arms of fans and at boundaries (Fig. 6b). At some places (Fig. 6c), the individual particles are arranged into arrays. Electron diffraction experiments proved the fans to be formed by coherent particles of the metastable $Al_3(Zr_xTi_{1-x})$ phase with the cubic $L1_2$ structure in the "cube to cube" orientation relationship to the matrix. The individual particles are probably formed by the same phase but they are not coherent with the matrix. The ratio of grains exhibiting the fan shaped precipitation decreases rapidly in the Al-Zr-Ti alloys with $x = 0.25$ and no fans were observed in the Al-Ti alloy (Fig. 6d). Only individual coarser particles were observed both within grains and at interfaces. The presence of Fe was proved in many of these particles.

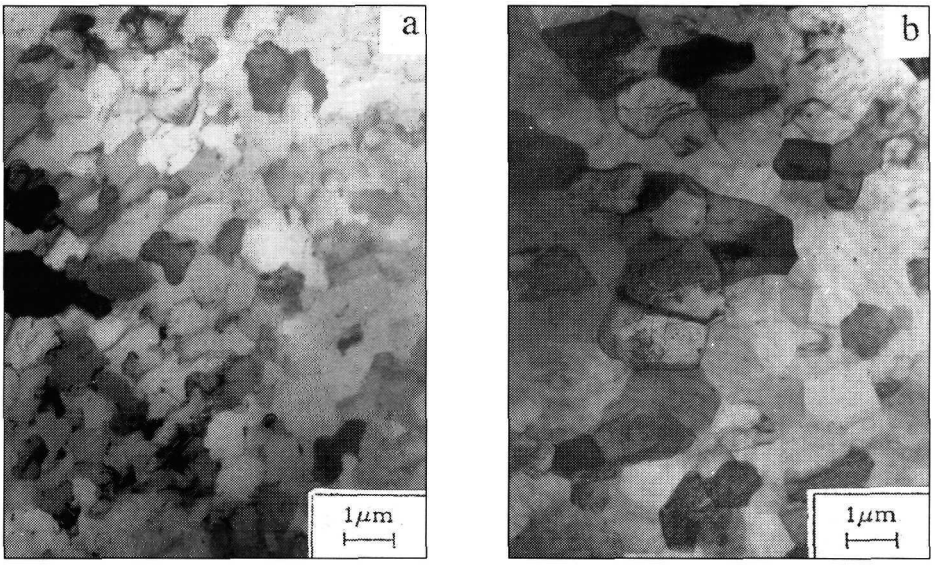

Fig. 5. The internal microstructure of the as melt-spun ribbons (TEM): a) $x = 0.5$, b) $x = 0$.

4. Discussion

The reason of a high strength of Al-based alloys containing Zr, V or Ti which were suggested as candidates for elevated temperature applications, should be a very dense distribution of small second phase particles formed due to a precipitation reaction in solid state. A microsegregation free solidification microstructure is a desirable precursor for this reaction. It was shown that such a solidification microstructure cannot be achieved using chill casting [11, 12]. Coarse petal-like particles composed of a dendritic structure of the $L1_2$ Al_3Zr or Al_3Ti phases and Al-based matrix were usually formed at the centres of grains [13, 14, 15]. A new way to a microsegregation free microstructure was opened by the development of rapid solidification techniques. Especially the melt spinning method characterised by cooling rates of about 10^6 $K \cdot s^{-1}$ is often used in laboratory experiments.

The solidification microstructure of as melt-spun ribbons of Al-based alloys consists generally of two zones [16]. The zone A adjoining the chilled surface of the ribbon exhibits usually a featureless microstructure if observed in light microscope. On the other hand, the zone B adjoining the free surface has typically a cellular or dendritic microstructure. A two-zone solidification microstructure was observed in our Al-Zr-Ti alloys, too. The zone A was found to be formed by columnar grains which are decomposed to a microcellular structure in Ti-rich alloys. This

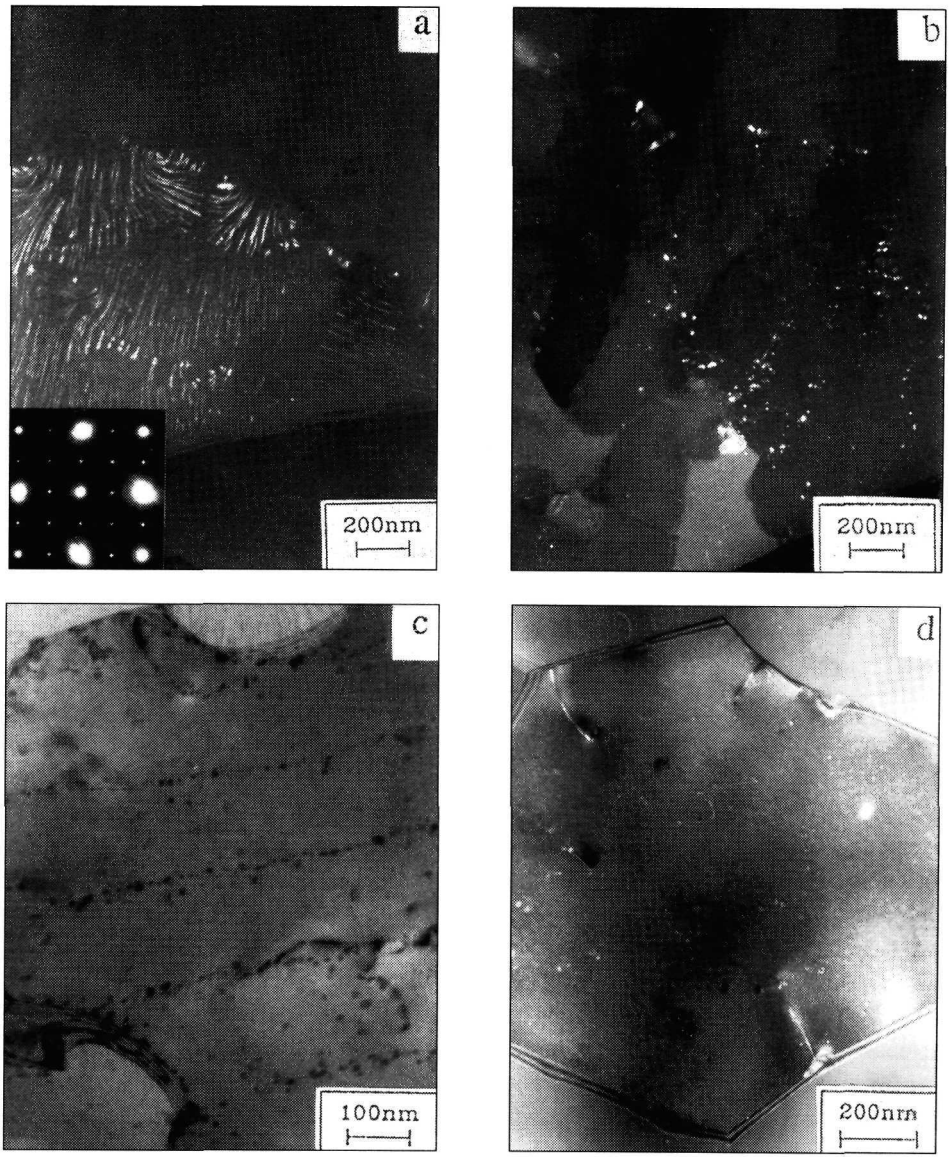

Fig. 6. The particles present in the as melt-spun ribbons (TEM): a) $x = 0.5$, dark field in (110) reflection of coherent $L1_2$ phase modification, b) $x = 0.5$, the same place, dark field in (111) reflection of non-coherent $L1_2$ phase modification, c) $x = 0.5$, d) $x = 0$.

result seems to be inconsistent with the above mentioned featureless microstructure. However, more detailed investigations of other Al-Zr-based alloys revealed similar

differences. Columnar grains were observed in Al-Zr-V alloys at places of a good contact of the melt with a wheel [17]. The cellular microstructure within grains was found both in binary Al-Zr alloys [18] and in Al-Zr-V alloys with a low V:Zr ratio [19]. Therefore, a fully microsegregation free solidification microstructure is not a general feature even at very high solidification rates.

The microstructure of the zone B was found to be cellular and dependent on the Zr:Ti ratio. An increasing amount of Ti favours unambiguously a formation of petal-like particles. This finding is in agreement with previous results in binary Al-Zr and Al-Ti alloys. In the Al-Zr alloys, the petal-like particles were found only at low solidification rates of the order of 10 $K \cdot s^{-1}$ [13, 14] and no such particles were observed in rapidly solidified alloys even at very high Zr contents (up to 8.6 wt.% [20]). On the other hand, the petal-like particles in Al-Ti alloys were observed even in melt-spun specimens [15, 21, 22]. It was shown that solidification rates of $2 \cdot 10^5$ and 10^6 $K \cdot s^{-1}$ are necessary to suppress the formation of petal-like particles in Al-Ti alloys the composition of which is close to our Ti-rich Al-Zr-Ti alloys ($x \leq 0.25$) [15]. These values are in good agreement with solidification rates expected at the free surface of melt-spun ribbons.

The $Al_3(Zr_xTi_{1-x})$ phase forms mostly fans composed of very small particles in the Zr-rich ($x \geq 0.5$) alloys. A similar microstructure was reported in as-melt-spun ribbons of the Al-3.3wt.%Zr [23] and Al-5vol.%$Al_3(Zr_{0.75}V_{0.25})$ [17] alloys. The fan shaped morphology is a typical feature in Al-Zr alloys aged at temperatures between 573 and 773 K [18, 20, 23, 24, 25]. In-situ TEM experiments performed in the Al-6%Zr alloy confirmed that this microstructure was formed by a discontinuous reaction [26]. The same mechanism seems to be operating also in our Zr-rich alloys. Fig. 6c shows the grain boundary bulges which extend alternatively into opposite grains, create undulations of the boundary and contribute to a significant curvature of boundaries. A proper investigation of the microstructure within boundary bulges revealed that all of them contained very fine particles arranged into fans.

The formation of fans is very limited in the alloy with $x = 0.25$ and fully suppressed in the binary Al-Ti alloy. The absence of discontinuous reaction results in straight grain boundaries. A similar absence of fans was observed in the V-rich Al-Zr-V alloys [17, 19] where only individual spherical particles were observed. A very low lattice mismatch between the Al_3(Zr,V) particles and Al-matrix in these V-rich alloys was believed to reduce the energy barrier for homogeneous nucleation of particles and to support the formation of individual particles rather than discontinuously formed fans. This explanation does not seem plausible with our experiments in Al-Zr-Ti alloys. The lowest lattice mismatch should be achieved in the Al-Zr-Ti alloy with $x = 0.75$, i.e. in the alloy where the fans are very frequent. On the other hand, the Ti-rich alloys which do not exhibit fan shaped microstructure have much worse lattice mismatch. We suppose that the difference between the structure of Zr-rich Al-Zr-Ti alloys and Ti-rich Al-Zr-Ti alloys (and probably

also V-rich Al-Zr-V alloys) is probably caused by significantly lower diffusion rate of Zr in Al as compared to that of V and Ti [27]. In the case of Zr, much faster kinetics of diffusion along grain boundaries favours the discontinuous reaction. A pinning effect of particles located at grain boundaries in Ti-rich and V-rich [19, 28] Al alloys may further suppress the migration of grain boundaries and, consequently, the discontinuous reaction.

The fans forming particles were found to be fully coherent with the Al-matrix. On the other hand, the individual particles seem to be only semicoherent. There may be two reasons for this orientation difference. Chen et al. [17] argued that the individual particles were originally formed in a coherent orientation which was distorted by the migration of the grain boundary during the discontinuous reaction. Another possibility is a preferential nucleation of these particles on dislocations, especially if the individual particles are arranged into arrays (see Fig. 6c). Similar bands within grains were observed in the microstructure of a rapidly solidified Al-6%Zr alloy [18] and interpreted as dislocations arrays. This observation may support the latter explanation.

The difference between the microhardness values of the as-melt-spun Zr-rich ($x \geq 0.5$) and Ti-rich ($x \leq 0.25$) Al-Zr-Ti alloys exceeds 100%. As the grain size and the solute content are nearly identical in both groups of alloys, the phase composition plays probably the decisive role in the explanation of the microhardness values. The *HK* values measured in the Ti-rich alloys are close to the value of the Vickers microhardness $HV = 59$ found in the as-melt-spun Al-3.9%Zr [20] and Al-0.54%Zr--2.23%V [29] alloys which have similar solute content as the alloys investigated in this study. Similarly to our Ti-rich alloys, the above mentioned alloys were found as nearly single-phase supersaturated solid solutions without the fan shaped arrangement of second phase particles. The main contribution to microhardness is probably given by solid solution strengthening in these materials.

The microhardness values measured in our as-melt-spun Zr-rich alloys are closer to values reported for alloys of similar composition after ageing. The peak microhardness values of $HV = 100$ [29] and 140 [20] were obtained in ribbons of Al--Zr alloys which should contain about 2.5 and 4.8 vol.% of the Al_3Zr phase in a fully decomposed state, respectively. In both these materials the fan shaped precipitation was developed. It can be concluded that the precipitation strengthening caused by the metastable coherent Al_3Zr particles is responsible for their high microhardness. Similar explanation seems to be valid also in our Zr-rich alloys. The comparison of our *HK* values with the literature data [20] enables to estimate roughly the volume fraction of the $Al_3(Zr_xTi_{1-x})$ in our Zr-rich alloys to be about 2%. This estimate agrees very well with the volume fraction resulting from our SAXS experiments [6].

A remarkable scatter of microhardness values was observed in the Zr-rich Al--Zr-Ti alloys with a tendency to lower *HK* values in thinner parts of ribbons and

in the zone adjoining the chilled surface. The WDA analysis proved the non-existence of significant composition gradient through the ribbons. The variations in *HK* reflect probably a difference in the phase composition, i.e. a different degree of decomposition at various places of ribbons. As the rates of solidification and subsequent cooling decrease with increasing distance from the chilled surface, a higher degree of decomposition is more probable in thicker parts of ribbons and in the zone adjoining the free surface. Therefore, higher values of microhardness can be expected at these places.

5. Conclusions

1. The solidification microstructure of the as-melt-spun Al-Zr-Ti ribbons is inhomogeneous along the direction perpendicular to the ribbon plane. Columnar grains were formed at the chilled surface of ribbons, whereas a microcellular structure with the cell size of about 1 μm is typical of the zone adjoining the free surface. Numerous petal-like particles were observed in the Ti-rich alloys.

2. The Ti-rich alloys ($x \leq 0.25$) are nearly single-phase. The grains are usually free of particles and few coarser particles found inside grains frequently contained Fe.

3. The Zr-rich alloys ($x \geq 0.5$) contain second phase particles of the size below 10 nm which are preferentially arranged into fans. These particles are fully coherent with the Al-matrix and were identified as the metastable $Al_3(Zr_xTi_{1-x})$ phase with the cubic $L1_2$ structure. Discontinuous reaction favoured by a slower diffusion rate of Zr in Al (as compared with Ti) is believed to be the reason for the formation of the fans in the Zr-rich alloys.

4. The microhardness values in the range of $HK = 48$ to 62 were found in the Ti-rich alloys. The main contribution is expected from solid solution strengthening.

5. Significantly higher microhardness values exceeding $HK = 100$ were found in Zr-rich alloys. The main strengthening effect is expected from the precipitates arranged into fans. The differences in microhardness values measured at different places of ribbons reflect probably the differences in the phase composition. The faster cooling rate at the chilled surface or at places of smaller ribbon thickness suppresses the decomposition of the supersaturated matrix and only solid solution strengthening contributes to the microhardness. The slower cooling rate near the free surface or at places of larger ribbon thickness enhances the precipitation of the metastable $Al_3(Zr_xTi_{1-x})$ phase which increases the microhardness values.

Acknowledgements

The authors are grateful to Dr. D. Plischke, Crystal Laboratory Göttingen, Germany, for the preparation of thin ribbons. The research was supported by the Grant Agency of the Charles University through the grant No. 283 and by the Grant Agency of the Czech Republic through the grant No. 93-2432. Alexander von Humboldt Foundation

has kindly donated the microhardness tester to the Department of Metal Physics of the Charles University, Prague.

REFERENCES

[1] SRINIVASAN, S.—DESCH, P. B.—SCHWARTZ, R. B.: Scripta Metall., *25*, 1991, p. 2513.
[2] NES, E.: Acta Metall., *20*, 1972, p. 499.
[3] MONDOLFO, L. F.: Aluminium Alloys: Structure and Properties. London, Butterworth 1976.
[4] DAS, S. K.—DAVIS, L. A.: Mater. Sci. Eng., *98*, 1988, p. 1.
[5] TSUNEKAWA, S.—FINE, M. E.: Scripta Metall., *16*, 1982, p. 391.
[6] MÁLEK, P.—BARTUŠKA, P.—PLEŠTIL, J.: Kovove Mater., *37*, 1999, p. 386.
[7] LIFSHITZ, I. M.—SLYOZOV, V. V.: J. Phys. Chem. Solids, 19, 1961, p. 35.
[8] WAGNER, C.: Z. Elektrochem., *65*, 1961, p. 581.
[9] JONES, H.: Aluminium, *54*, 1978, p. 274.
[10] JONES, H.: Rapid Solidification of Metals and Alloys. London, Inst. of Metallurgists 1982.
[11] OHASHI, T.—ICHIKAWA, R.: Met. Trans., *3*, 1972, p. 2300.
[12] NES, E.—BILLDAL, H.: Acta Metall., *25*, 1977, p. 1039.
[13] OHASHI, T.—ICHIKAWA, R.: Z. Metallkde., *61*, 1973, p. 517.
[14] NES, E.—BILLDAL, H.: Acta Metall., *25*, 1977, p. 1031.
[15] HORI, S.—TAI, H.—NARITA, Y.: Microstructure of rapidly solidified Al-Ti alloys containing titanium up to 40 % and its thermal stability. In: Rapidly Quenched Metals. Eds.: Steeb, S., Warlimont, H. Elsevier Sci. Publ. 1985, p. 911.
[16] JONES, H. : Mater. Sci. Eng., *5*, 1969/70, p. 1.
[17] CHEN, Y. C.—FINE, M. E.—WEERTMAN, J. R.: Acta Metall. Mater., *38*, 1990, p. 771.
[18] PANDEY, S. K.—GANGOPADHYAY, D. K.—SURYANARAYANA, C.: Z. Metallkde., *77*, 1986, p. 12.
[19] LEWIS, R. E.—CROOKS, D. D.—CHEN, Y. C.—FINE, M. E.—WEERTMAN, J. R.: In: Proc. 3rd Int. Conf. on Creep and Fracture of Eng. Mater. Eds.: Wilshire, B., Evans, R. W. London, The Inst. of Metals 1987, p. 331.
[20] SAHIN, E.—JONES, H.: Extended solid solubility, grain refinement and age hardening in Al-1 to 13 wt.% Zr rapidly quenched from the melt. In: Rapidly Quenched Metals III. Ed.: Cantor, B. London, The Metals Soc. 1978, p. 138.
[21] MAJUMDAR, A.—MUDDLE, B. C.: Mater. Sci. Eng. A, *169*, 1993, p. 135.
[22] CHU, M. G.: Mater. Sci. Eng. A, *179/180*, 1994, p. 669.
[23] OCTOR, H.—NAKA, S.: Phil. Mag. Letters, *59*, 1989, p. 229.
[24] ZEDALIS, M.—FINE, M. E.: Met. Trans. A, *17*, 1986, p. 2187.
[25] RYUM, N.: Acta Metall., *20*, 1969, p. 499.
[26] CHAUDHURY, Z. A.—SURYANARAYANA, C.: Metallography, *17*, 1984, p. 231.
[27] LEE, H. M.: Scripta Metall. Mater., *24*, 1990, p. 2443.
[28] CHEN, Y. C.—FINE, M. E.—WEERTMAN, J. R.—LEWIS, R. E.: Scripta Metall., *21*, 1987, p. 1003.
[29] PARK, W.-W.—KIM, T.-H.: Scripta Metall., *22*, 1988, p. 1709.

Received: 19.4.1999